Variable temperature neutron powder diffraction study to determine the magnetic interactions in Sr_2LnRuO_6 (Ln = Ho and Tb)

2004 J. Phys.: Condens. Matter 16 7611

(http://iopscience.iop.org/0953-8984/16/43/005)

INSTITUTE OF PHYSICS PUBLISHING JOURNAL OF PHYSICS: CONDENSED MATTER

J. Phys.: Condens. Matter **16** (2004) 7611–7624 PII: S0953-8984(04)79836-7

Variable temperature neutron powder diffraction study to determine the magnetic interactions in Sr_2LnRuO_6 (Ln = Ho and Tb)

Neil G Parkinson[1,2], Peter D Hatton[2], Judith A K Howard[1], Clemens Ritter[3], Richard M Ibberson[4] and Maw-Kuen Wu[5]

[1] Department of Chemistry, University of Durham, Durham DH1 3LE, UK
[2] Department of Physics, University of Durham, Durham DH1 3LE, UK
[3] Institut Laue-Langevin, BP 156, F-38042 Grenoble Cedex 9, France
[4] ISIS Facility, Rutherford Appleton Laboratory, Didcot OX11 0QX, UK
[5] Department of Physics and Materials Centre, National Tsing Hua University, Hsinchu, Taiwan

E-mail: p.d.hatton@durham.ac.uk

Received 23 April 2004, in final form 22 July 2004
Published 15 October 2004
Online at stacks.iop.org/JPhysCM/16/7611
doi:10.1088/0953-8984/16/43/005

Abstract

Neutron powder diffraction has been used to study the two title compounds, Sr_2HoRuO_6 and Sr_2TbRuO_6, in order to determine the crystal and magnetic structures of the materials. Both materials have a distorted double perovskite structure and at temperatures below 30–40 K long-range magnetic order is observed. The magnetic structure for each compound consists of two interpenetrating Type I arrangements, one for the ruthenium sublattice and one for the rare earth sublattice, which are antiferromagnetically coupled to each other and order at the same temperature. From variable temperature measurements the combination of magnetic interactions and their relative strengths was deduced. The antiferromagnetic Ru–O–O–Ru interaction is approximately constant in the compounds, but it is a factor of 2.5 and 0.7 times stronger than the antiferromagnetic Ru–O–Ho and Ru–O–Tb interactions respectively.

1. Introduction

There have been extensive studies of the ruthenate double perovskites with the general formula of $A_2B'RuO_6$ (A = alkaline earth element, B′ = transition metal or rare earth element) due to the intriguing magnetic behaviour of the Ru^{5+} ion [1–3]. Crystallographic ordering of the B cations, B′ and Ru^{5+}, is essential for the development of long-range magnetic order in the materials, while the competition between those magnetic interactions present must not be too great, otherwise a spin glass may form.

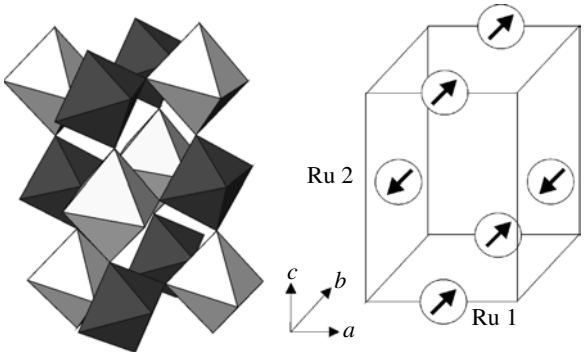

Figure 1. The crystal structure of an ordered double perovskite such as Sr_2YRuO_6, with a crystal unit cell of $\sim\sqrt{2}a_p \times \sqrt{2}a_p \times 2a_p$, where a_p is the lattice parameter of a simple cubic perovskite. Oxygen octahedra surround both the Ru^{5+} ions (dark) and Y^{3+} ions (light), while the Sr^{2+} ions are not shown for clarity. The Type I antiferromagnetic structure shares the same unit cell as the crystal structure and has the magnetic moment orientated in opposite directions on the two Ru^{5+} sites.

The choice of a large diamagnetic ion, such as Y^{3+} or Lu^{3+}, for the B′ cation ensures that the B cations are crystallographically ordered [4] and that the magnetic interactions which arise are due to the Ru^{5+} ion only. This simple magnetic behaviour in $A_2B'RuO_6$ (A = Sr or Ba, B′ = Y^{3+} or Lu^{3+}) [1, 5] manifests itself with the ruthenium sublattice adopting a Type I antiferromagnetic arrangement, as shown in figure 1. The magnetic ordering is via the Ru–O–O–Ru interaction and there is negligible interaction from the Ru–O–Y–O–Ru pathway as the Y^{3+} (or Lu^{3+}) is fully ionized. However, when transition metals are used no long-range magnetic order is observed due to the crystallographic disorder of the B cations arising from their similar charges and sizes. This is illustrated with the example of Sr_2FeRuO_6, which would order in a ferromagnetic structure due to the ferromagnetic Ru–O–Fe interaction if the B cations were ordered. However, there is a random distribution of B cations and this leads to the presence of antiferromagnetic Ru–O–Ru and Fe–O–Fe interactions also, which leads to the development of a spin glass [2].

The initial study of A_2LnRuO_6 (A = Ca or Sr, Ln = rare earth) by Battle shows that for a rare earth element to fully occupy a B site, the A cation must not be too small in comparison [6]. This condition is always satisfied in the systematic study by Doi and Hinatsu of Sr_2LnRuO_6 [7] (Ln = Eu–Lu), and the Ln^{3+} rare earth ions are still sufficiently large compared to the Ru^{5+} ions to ensure crystallographic ordering of the B cations. Thus, the magnetic interactions of Ru^{5+} with 4f systems are easier to study because the only interactions present in the A_2LnRuO_6 materials are the nearest-neighbour (NN) interaction of Ru–O–Ln and the next-nearest-neighbour (NNN) interactions of Ru–O–O–Ru and Ln–O–O–Ln. In the study by Battle of Sr_2ErRuO_6 [6] the Ru^{5+} and Er^{3+} sublattices each adopt a Type I antiferromagnetic structure, with the interaction between the rare earths reasoned to be negligibly weak due to the very low Néel temperature of 3.4 K in Er_2O_3. The Ru–O–O–Ru interaction is responsible for the magnetic ordering in the ruthenium sublattice, while the Ru–O–Er interaction yields the complementary magnetic structure of the Er^{3+} sublattice.

In this paper high-resolution neutron powder diffraction patterns of Sr_2HoRuO_6 have been measured on HRPD at ISIS to study the crystal structure in fine detail through the magnetic ordering temperature. Variable temperature neutron powder diffraction patterns were measured at the high-flux instrument D1B at the ILL for both the Sr_2HoRuO_6 and Sr_2TbRuO_6 samples in order to determine the magnetic structure and its development with temperature.

The information obtained was sufficient for determining the magnetic interactions present within the materials.

2. Experimental details

The samples of Sr_2LnRuO_6 (Ln = Ho or Tb) were prepared by a solid-state reaction method with the stoichiometric amounts of Ln_2O_3, RuO_2 and $SrCO_3$ which were mixed and calcined at 1000 °C for several days. The reacted powders were sintered at 1375 °C in an atmosphere of 70% oxygen and 30% argon for 12 h, and annealed for a further 12 h. X-ray diffraction measurements were then used to verify that the reaction was complete or the heating cycle would be repeated. For each sample 3–4 g of powdered material were produced.

Neutron powder diffraction patterns were measured at HRPD (ISIS) at 5, 20 and 50 K for the Sr_2HoRuO_6 sample for 7 h each. This enabled the d-spacing region of 1–3 Å to be examined with excellent resolution of $\Delta d/d \sim 4 \times 10^{-4}$ and allowed accurate crystal structure refinement.

The high-flux diffractometer D1B (ILL) has a 80° wide detector bank consisting of 400 detectors spaced every 0.2°. The detector bank was fixed between 5° and 85°, with a wavelength of 2.524 Å, which allowed the measurement of the magnetic peaks. The temperature was increased at a rate of 0.2 K min^{-1} from 2 to 50 K and a pattern collected every 10 min for both samples, which enabled the magnetic structures to be determined throughout the entire temperature region of interest. This strategy, rather than a sequence of fixed temperature steps, ensured maximal use of beam-time, without significant loss of accuracy of temperature for each individual diffraction pattern. In fact, the transition temperatures are better determined by this strategy as a greater number of temperatures can be measured in the same amount of beam-time. The heating rate of 0.2 K min^{-1} was not too fast as a select number of fixed temperature measurements yielded data and results in full accord with those obtained using this variable temperature method. For all neutron diffraction experiments at HRPD and D1B the samples were contained in 6 mm radius vanadium cans.

3. Results and discussion

3.1. Crystal structures

The diffraction pattern of Sr_2HoRuO_6 measured at 50 K, which these neutron diffraction experiments determine to be above the magnetic ordering temperature, using HRPD is shown in figure 2. The refinements were performed using GSAS [8] in space group $P2_1/n$ assuming a 1:1 ordering of the Ru^{5+} and Ho^{3+} cations as would be expected from their charge and size. This requires the crystal structure unit cell for the distorted double perovskite to be $\sim\sqrt{2}a_p \times \sqrt{2}a_p \times 2a_p$, where a_p is the lattice parameter of a simple cubic perovskite. The diffraction pattern has been shown in two sections simply to emphasize both the high quality and resolution of the data measured at HRPD, even at these low d-spacings, and also, the comparable standard of the crystal model used to calculate the diffraction profile. There is no significant mismatch between the observed intensity and the calculated profile, which is generated from the model crystal structure in table 1. The bond lengths and angles calculated from this are listed in table 2 and the crystal structure is shown in figure 3. The tilting of the oxygen octahedra highlights the deviation of the Ru–O–Ho bond angles to 154°–158°. The refinements of the 2 and 20 K crystal structure of Sr_2HoRuO_6 did not vary too greatly from the 50 K structure, and in particular the important Ru–O–Ho bond angles remained within this stated bound. These results are in agreement with a previous study of Sr_2HoRuO_6 by Doi *et al* [9].

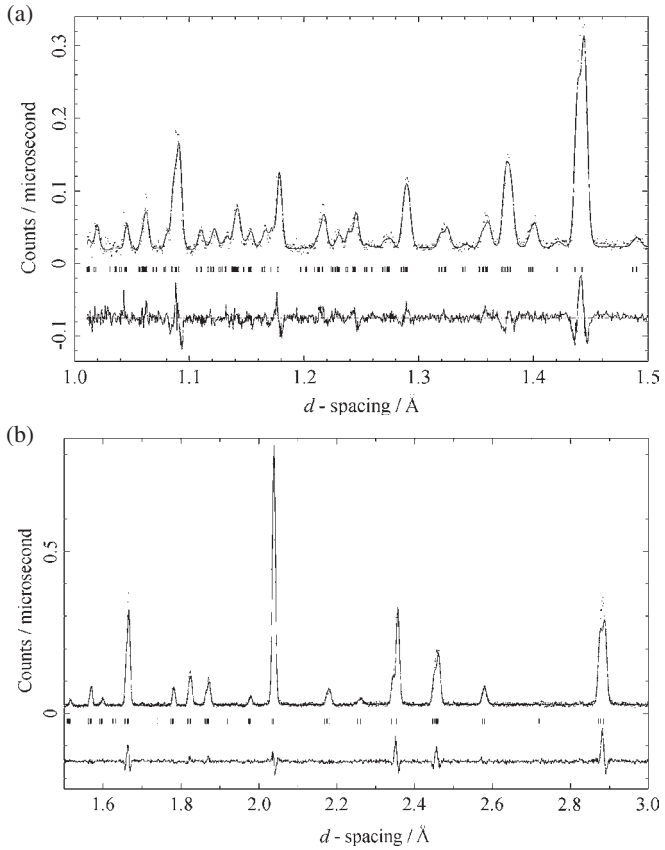

Figure 2. The diffraction pattern of Sr_2HoRuO_6 measured at 50 K using HRPD and shown in two sections, 1–1.5 and 1.5–3 Å. The observed data points are shown as crosses, with the calculated profile and difference curve as lines. The tick marks denote allowed crystal structure reflections.

Table 1. The refined lattice parameters and atomic coordinates of Sr_2HoRuO_6 at 50 K obtained using HRPD data.

Sr_2HoRuO_6	$P2_1/n$					
a (Å)	b (Å)	c (Å)	β (deg)			
5.757 35(5)	5.776 40(5)	8.142 02(14)	90.356(1)			
Atom	Site	x	y	z	Occ.	β (Å^2)
Sr	4e	0.0075(16)	0.0306(7)	0.7552(11)	1.00	0.30(3)
Ho	2c	0	1/2	0	1.00	0.20(9)
Ru	2d	1/2	0	0	1.00	0.38(10)
O1	4e	0.3015(15)	0.2776(14)	0.9605(9)	1.00	0.35(10)
O2	4e	0.2667(12)	0.2935(14)	0.5403(11)	1.00	0.42(12)
O3	4e	0.9329(14)	0.4809(11)	0.7304(8)	1.00	0.27(7)
$R_p = 10.59\%$, $R_{wp} = 12.70\%$, $R_{exp} = 7.84\%$, $R_{F^2} = 7.75\%$						

No high-resolution neutron diffraction data were available for Sr_2TbRuO_6, but from a previous study of Sr_2LnRuO_6 (Ln = Ho and Tb) [10], the crystal structures were determined to be virtually identical except for the slighter larger lattice parameters of the Tb analogue.

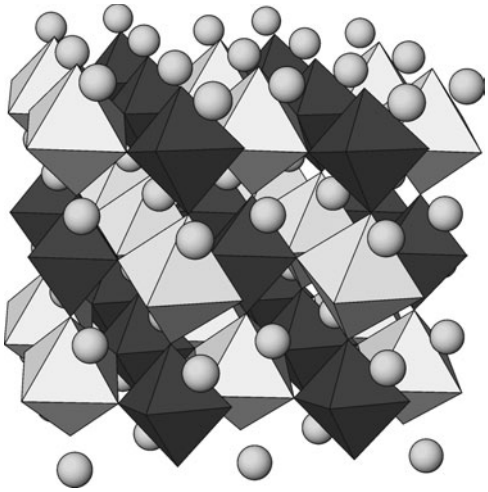

Figure 3. The refined crystal structure of Sr_2HoRuO_6, which is a distorted double perovskite. The RuO_6 octahedra (dark) and the HoO_6 octahedra (light) are shared at the corners and form an ordered 1:1 arrangement. The distortion manifests with the tilting of the octahedra, whereas the strontium, which is shown as light circles, occupies the space between the octahedra.

Table 2. Principal bond lengths (Å) and angles (deg) for Sr_2HoRuO_6.

Sr_2HoRuO_6 at 50 K										
Ho–O(1)	2.185(9)	Ru–O(1)	1.994(8)	O(1)–Ho–O(2)	93.2(4)	O(1)–Ru–O(2)	90.8(5)	Ru–O(1)–Ho	154.7(4)
Ho–O(2)	2.189(7)	Ru–O(2)	1.970(7)	O(1)–Ho–O(3)	92.4(3)	O(1)–Ru–O(3)	90.4(4)	Ru–O(2)–Ho	157.2(5)
Ho–O(3)	2.230(7)	Ru–O(3)	1.920(7)	O(2)–Ho–O(3)	90.4(3)	O(2)–Ru–O(3)	92.1(5)	Ru–O(3)–Ho	157.5(5)

Thus, for the refinement of Sr_2TbRuO_6 (and Sr_2HoRuO_6) using data measured at D1B, the atomic coordinates and thermal parameters for Sr_2HoRuO_6 were used from table 1. This would result in no loss of accuracy of the refinements of the lattice parameters (or magnetic moment) as D1B is not sensitive to crystal structure changes on such a small scale as the resolution is lower and there are fewer peaks in the pattern because each only extends to $(\sin\theta)/\lambda \sim 0.27$ Å^{-1}. Figure 4 shows the diffraction pattern of Sr_2TbRuO_6 measured at 50 K using D1B with the calculated profile, which is virtually identical to that of Sr_2HoRuO_6, and the similarity of the two further validates this approach. The feature at $2\theta \sim 72°$ was not in diffraction patterns measured using other diffractometers, though it was present in all those measured at D1B as it originates from the vanadium of its cryostat, rather than from the sample. The unit cell parameters for both compounds at 50 K are given in table 3, which confirms the larger size of the unit cell for Sr_2TbRuO_6. The unit cell parameters for Sr_2HoRuO_6 are $\sim 3\sigma$ from the HRPD values, which is taken as the standard for comparing unit cell parameters from different diffractometers, and so are in reasonable agreement. For both compounds, all the diffraction patterns measured at D1B between 2 and 50 K were refined with similar *R*-factors (with $R_p \sim 2.2\%$, $R_{wp} \sim 3.1\%$, $R_{exp} \sim 1.7\%$, $R_{F^2} \sim 3.9\%$,) and there was no significant change in the unit cell parameters in this temperature region.

3.2. Magnetic structures

3.2.1. Determining the starting model from the data. The variable temperature neutron powder diffraction patterns measured at D1B for Sr_2HoRuO_6 and Sr_2TbRuO_6 are shown in

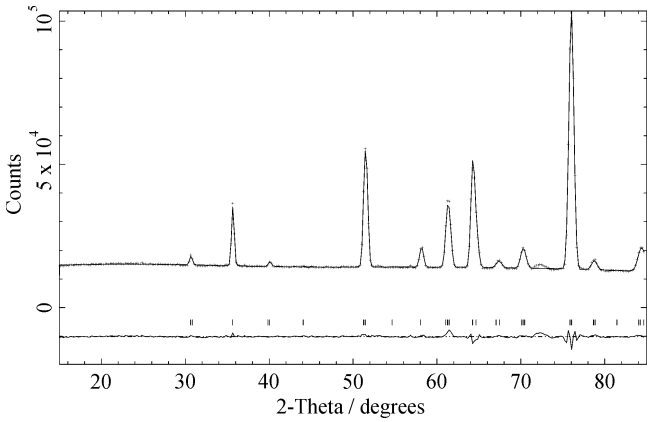

Figure 4. The diffraction pattern of Sr_2TbRuO_6 measured at 50 K using D1B. The data points are shown as crosses and the calculated profile and difference curve as lines. The tick marks indicate the positions of allowed crystal structure reflections.

Table 3. The refined lattice parameters of Sr_2HoRuO_6 (shown in bold) and Sr_2TbRuO_6 at 50 K obtained using D1B data.

a (Å)	b (Å)	c (Å)	β (deg)
5.756 91(13)	**5.775 96(13)**	**8.140 55(36)**	**90.355(2)**
5.788 62(10)	5.814 75(13)	8.200 16(28)	90.402(2)

figure 5, and due to their similarity, much of the discussion can be shared. At temperatures below 30–40 K extra peaks appear in the diffraction patterns indicating the onset of long-range magnetic order in the materials. As the location of the magnetic intensity in the diffraction patterns is not primarily coincident with the existing crystal structure peaks, this indicates that there is long-range antiferromagnetic order. The magnetic intensity can be indexed with $h+k+l$ being odd, the reflection condition for an antiferromagnetic structure, when the magnetic unit cell is chosen to be the same size as the crystal structure unit cell. With this size of magnetic unit cell, the only antiferromagnetic structure allowed is Type I, as Type II and Type III require larger magnetic unit cells [5]. The Ru^{5+} and Ln^{3+} ions may each adopt a Type I antiferromagnetic structure which can interpenetrate in one of the two ways illustrated in figure 6.

With the magnetic unit cell determined, the first two magnetic peaks in the diffraction patterns are indexed as the (001) reflection, and the unresolved combination of the (100) and (010) reflections. The presence of a magnetic peak indicates that a component of the magnetic moment is perpendicular to the direction of the scattering vector. Thus, the small (001) peak indicates a small component of the magnetic moment in the ab plane. As the unresolved combination of the (100) and (010) reflections is large, while the (001) is not, this suggests that the majority of the magnetic moment lies in the c-direction. As the (001) magnetic peak is only observable up to 9 K in Sr_2HoRuO_6 and 25 K in Sr_2TbRuO_6, this suggests that the ab component is only measurable explicitly below these temperatures.

The diffraction patterns of Sr_2HoRuO_6 and Sr_2TbRuO_6 measured at 2 K using D1B are shown in figure 7. The lower set of tick marks denote the crystal structure reflections, whereas the upper set mark the possible magnetic reflections using the same unit cell parameters but space group $P\bar{1}$. The magnetic peaks indicated by arrows are composed of reflections where $h+k+l$ is odd. These antiferromagnetic peaks can be further divided into two groups: those

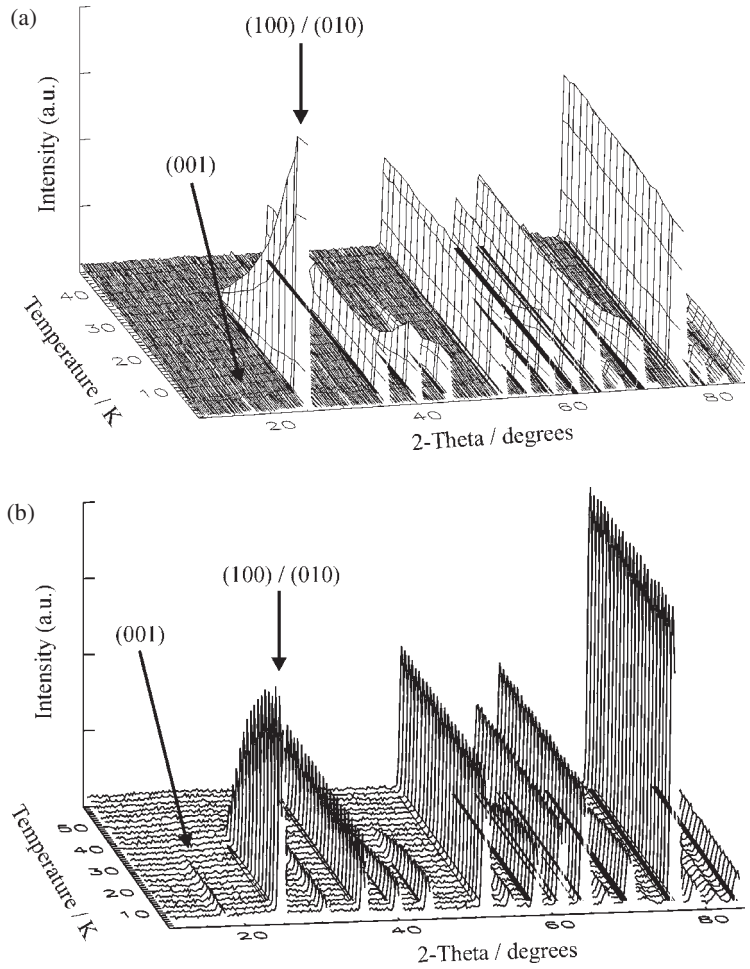

Figure 5. The variable temperature neutron powder diffraction patterns of (a) Sr_2HoRuO_6 and (b) Sr_2TbRuO_6 measured at D1B from 2 to 50 K. The extra peaks in the diffraction patterns below 30–40 K are of magnetic origin and the (001) and the unresolved combination of the (100) and (010) are explicitly indexed. The crystal structure peaks do not change significantly and indicate that there is no major structural change through the magnetic transition.

where $h + k$ is odd and l is even are additionally marked with an asterisk, while those where $h + k$ is even and l is odd receive no further marking.

The relative orientations of the two magnetic sublattices, illustrated in figure 6, determine which group of peaks is formed from the sum of the magnetic moments of Ru^{5+} and Ln^{3+}, and the other group formed from the difference. Clearly, as the sum and difference magnetic peaks are not the same size, neither of the Ru^{5+} and Ln^{3+} magnetic moments can be zero, confirming that each sublattice does order in a Type I antiferromagnetic structure. As the magnetic peaks which are asterisked are larger throughout the diffraction pattern than those which are not, those magnetic peaks where $h + k$ is odd and l is even are formed from the sum of the magnetic moments. Consultation of table 4 requests that the two sublattices are anti-parallel to each other, and indicates that the Ru–O–Ln interaction is antiferromagnetic.

Except for the (001) magnetic peak which is small due to the direction of the magnetic moments, the magnetic peaks formed from the sum of the magnetic moments are larger but

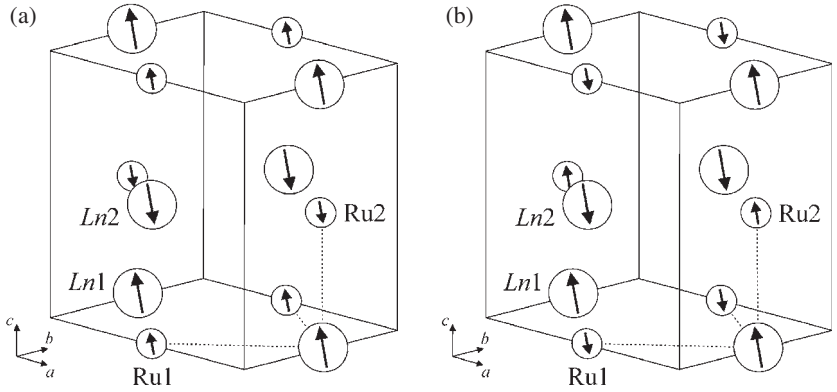

Figure 6. The Ru^{5+} and Ln^{3+} ions each form Type I magnetic sublattices. The two sublattices couple (a) ferromagnetically and (b) ferrimagnetically. The *inter-species* interaction is shown by the dotted lines and its nature is most easily seen from the directions of the moments in the *ab* plane, which are parallel and anti-parallel respectively. In both cases only four out of the six NN *inter-species* interactions are satisfied. The moments are shown at a slight inclination from the *c*-axis.

Table 4. The magnitude of the reflections is governed by the *inter*-species coupling as indicated from the sum and difference peaks.

	Lattices parallel		Lattices anti-parallel	
	Ferromagnetic		Ferrimagnetic	
Type of reflection	$(h+k)$	l	$(h+k)$	l
Sum	Even	Odd	Odd	Even
Difference	Odd	Even	Even	Odd

still have the same order of magnitude compared to those formed from the difference. As the magnetic intensity is proportional to the square of these resultant moments, this implies that there is a large difference in size of the magnetic moments of the Ru^{5+} and Ln^{3+} ions. The rare earth is expected to have a large magnetic moment, accounting for the extremely high level of magnetic intensity in the diffraction pattern, which is comparable to the crystal structure intensity in both Sr_2HoRuO_6 and Sr_2TbRuO_6. The Ru^{5+} magnetic moment is expected to be $\sim 2\ \mu_B$ from previous studies of the ruthenates [1, 5, 6, 11].

The magnetic form factors of both the Ho^{3+} and Tb^{3+} ions are listed in *The International Tables of Crystallography* [12], but the Ru^{5+} ion is not included. The closest ruthenium species which are included are Ru and Ru^{+}, so some previous studies [3, 9, 13, 14] have used Zr^{+}, as this is isoelectronic with Ru^{5+}. However, recently an empirical magnetic form factor for Ru^{5+} has been determined [15] which allows accurate refinement of the magnetic moment. The primary contribution to the magnetic form factor results from the spatial extent of the electrons responsible for the magnetic properties, and this can be compared for Ru^{+}, Zr^{+} and with the recent calculation for Ru^{5+}. The Zr^{+} ion is larger than the Ru^{+} ion and so the magnetic form factor of the former species decreases more quickly with $(\sin\theta)/\lambda$. However, the Ru^{5+} ion is smaller than the Ru^{+} ion and so the magnetic form factor should decrease more slowly. As the calculated magnetic form factor of the Ru^{5+} ion has this correct dependence, whereas the isoelectronic Zr^{+} ion does not, it has been used for all the refinements in this study.

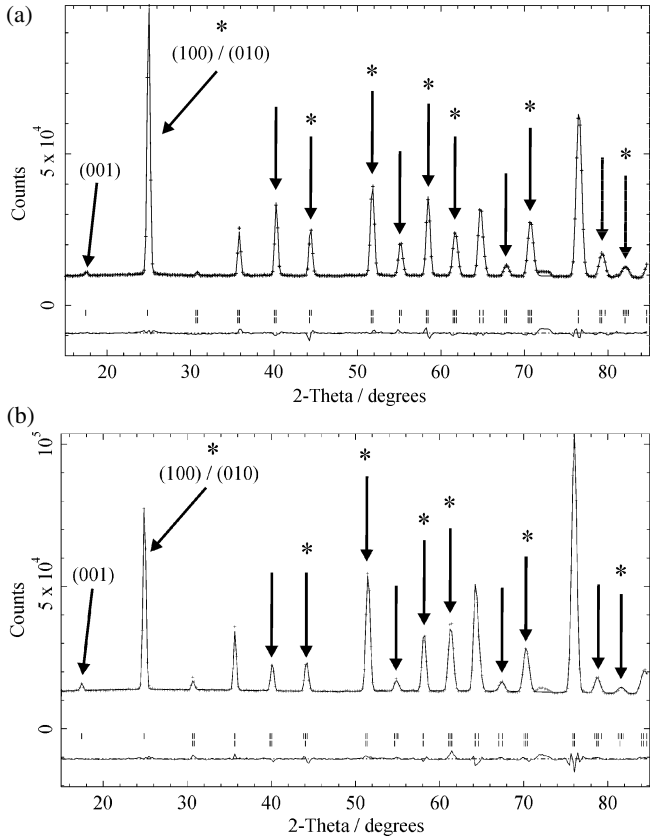

Figure 7. The diffraction patterns of (a) Sr_2HoRuO_6 and (b) Sr_2TbRuO_6 measured at 2 K using D1B. The data points are marked by crosses, while the calculated profile and difference curve are solid lines. The lower set of tick marks denote the crystal structure reflections. The upper set denote possible magnetic structure reflections, but the arrows only denote antiferromagnetic peaks. Those where $h + k$ is odd and l is even are marked with an asterisk, while those where $h + k$ is even and l is odd are unmarked. The (001) and unresolved combination of the (100) and (010) are explicitly indexed.

This piece of information is the final contribution to the starting model of the magnetic structure, which has been determined from the experimental observations, and contains all the necessary elements for refinement. Both the Sr_2HoRuO_6 and Sr_2TbRuO_6 magnetic structures were refined with sublattices of Ru^{5+} and Ln^{3+} ions each adopting Type I antiferromagnetic structures, which were coupled ferrimagnetically. The magnetic moments of the ions were refined primarily in the c-direction, with the ab component only measurable at the lowest temperatures. The magnetic moment of Ru^{5+} was initially refined from $\sim 2\ \mu_B$ and Ho^{3+} was initially set at $\sim 9\ \mu_B$, approaching its theoretical value, while $\sim 6\ \mu_B$ was chosen for Tb^{3+} as there is less magnetic intensity in the Sr_2TbRuO_6 data.

3.2.2. Refinement results. The diffraction profile calculated from the refined magnetic structure of Sr_2HoRuO_6 at 2 K is shown in figure 7(a) and replicates the data well, with R-factors of $R_p = 2.06\%$, $R_{wp} = 3.06\%$, $R_{exp} = 0.87\%$ and $R_{F^2} = 3.75\%$. The c components of the magnetic moments of Ru^{5+} and Ho^{3+} are refined to be 1.79(9) μ_B and 7.87(4) μ_B respectively.

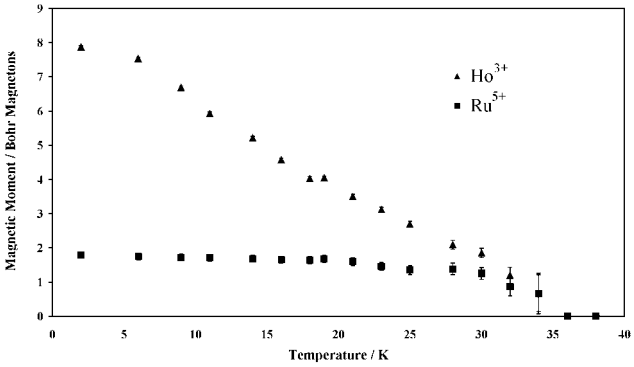

Figure 8. The magnitude of the magnetic moment of Ru^{5+} and Ho^{3+} in the *c*-direction with temperature. For Sr_2HoRuO_6 the two sublattices are anti-parallel to each other.

However, the refinements proceed equally well with a small 0.97(12) μ_B component in the *ab* plane on either ion. This *ab* component was finally assigned predominantly to the Ho^{3+} ion from consideration of the temperature dependence of the magnetic moments. The *ab* component required on the Ru^{5+} ion, to maintain collinearity, is sufficiently small to be neglected in the refinement and so both the magnetic moments of the Ru^{5+} and Ho^{3+} ions are at $\sim 7^\circ$ from the *c*-axis, as illustrated in figure 6(b).

Each diffraction pattern of Sr_2HoRuO_6 between 2 and 50 K was refined and the magnetic moments of the Ru^{5+} and Ho^{3+} ions are displayed in figure 8. As the *ab* component is only $\sim 1\ \mu_B$ below 9 K, while the *c* component of Ho^{3+} is $\sim 8\ \mu_B$, figure 8 effectively shows the total magnetic moments in the system. The ordered Ru^{5+} magnetic moment is approximately constant at 1.7(1) μ_B up to 20 K, then decreases with $T_N \sim 34$ K. The Ho^{3+} magnetic moment shares the same magnetic ordering temperature of 34 K, but orders only gradually, until it finally saturates at ~ 4 K.

The refined *ab* component of the magnetic moment is $\sim 1\ \mu_B$ for all temperatures below 9 K, while for this combination of diffractometer and amount of this sample the sensitivity is $\sim 0.8\ \mu_B$. Although the loss of the (001) peak could indicate a spin reorientation with the moments above 9 K being aligned purely in the *c*-direction, it is also possible that there is still a small magnetic moment in the *ab*-direction, though this is now too small to be measured. If the magnetic moment in the *ab* plane has a similar temperature dependence to the *c*-direction one, it is likely that it is predominantly due to the Ho^{3+} ion as mentioned above.

In order to determine the direction of the magnetic moments in the *ab* plane, the (100) and (010) reflections would have to be resolved as two peaks. The intensity of a magnetic peak is proportional to the square of the magnetic moment which is perpendicular to the scattering vector. The sum of the magnetic moments in the *c*-direction is $\sim 10\ \mu_B$, whereas the *ab* component is $\sim 1\ \mu_B$. So the difference in intensities of the (100) and (010) would be only 1% if the moment in the *ab* plane was directed along either of the two axes, *a* or *b*. This difference would be even less for intermediate angles in the *ab* plane, so it is not possible to draw any further conclusions about the moment direction in the *ab* plane.

The magnetic structure of Sr_2TbRuO_6 was refined similarly, with the calculated profile for the 2 K data shown in figure 7(b). Again the *R*-factors are low with $R_p = 1.86\%$, $R_{wp} = 2.63\%$, $R_{exp} = 0.76\%$ and $R_{F^2} = 4.28\%$ and the refined *c* components of the magnetic moments of Ru^{5+} and Tb^{3+} are 1.91(10) μ_B and 4.54(4) μ_B respectively. Again, the magnetic moment of 1.17(8) μ_B in the *ab* plane is small and largely attributable to the rare earth ion, leading to a deviation of $\sim 14^\circ$ from the *c*-axis of the moments, as in figure 6(b).

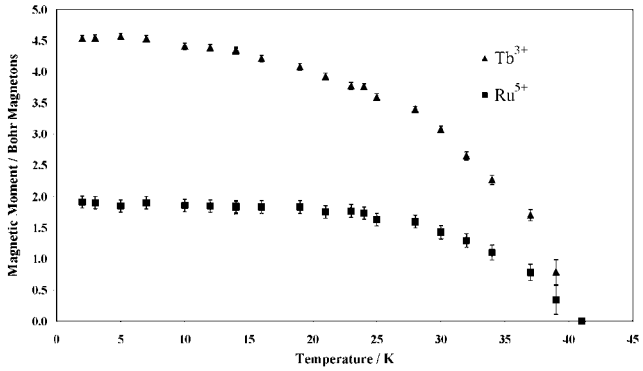

Figure 9. The magnetic moment in the *c*-direction for the Ru^{5+} and Tb^{3+} ions with temperature.

The variation with temperature of the magnetic moments in the *c*-direction is shown in figure 9 for Sr_2TbRuO_6. The magnetic moment of the Ru^{5+} ion behaves very similarly in Sr_2TbRuO_6 and Sr_2HoRuO_6, except that the moment appears to saturate and begin to order at the higher temperatures of ∼25 and 39 K respectively in the Tb analogue. Again the ordering temperatures of the two ions are coincident, but the Tb^{3+} magnetic moment orders at a similar rate to the Ru^{5+} ordered magnetic moment and saturates at ∼14 K. This contrasts with the behaviour of the Ho^{3+} magnetic moment, which ordered more gradually and only saturated at the much lower temperature of ∼4 K. The refined *ab* component was approximately constant at ∼1.1 μ_B, up to 20 K, before becoming too small to measure above 25 K, imitating the Tb^{3+} magnetic moment in the *c*-direction.

Earlier neutron diffraction studies by Doi and Hinatsu of Sr_2HoRuO_6 [9] and Sr_2TbRuO_6 [13] measured neutron diffraction patterns at room temperature and 10 K, and additionally for the Ho analogue at 25 K. The refined magnetic structures are broadly similar, though the magnetic moment sizes differed significantly in some cases. The refinements using 10 K data can be compared and their studies determined the magnetic moments of Ho^{3+} and Tb^{3+} to be 6.66(8) μ_B and 4.98(12) μ_B respectively, while this study proposes 6.68(5) μ_B and 4.56(4) μ_B. The magnetic moments of the Ho^{3+} ions are in good agreement, particular considering its rate of change with temperature at 10 K, whereas there is a slight discrepancy between the values for the Tb^{3+} ions. More alarming is the overestimation of the Ru^{5+} magnetic moment, which they report as 2.74(9) μ_B and 2.99(11) μ_B in the Ho and Tb materials respectively, whereas this study indicates 1.72(10) μ_B and 1.86(10) μ_B, values more in keeping with the rest of the literature [1, 5, 6, 11].

This overestimation can be attributed to their use of the Zr^+ magnetic form factor, rather than the calculated Ru^{5+} magnetic form factor used here. For the rare earth ruthenates studied here, there is a large amount of magnetic intensity at high angles. The Zr^+ magnetic form factor decreases much more rapidly than Ru^{5+} with increasing $(\sin\theta)/\lambda$. So using Zr^+ will require successively larger magnetic moments to replicate the magnetic intensity when more magnetic peaks appear at high angles. Considering only the largest magnetic peak in the pattern, formed from the (100) and (010) reflections at $(\sin\theta)/\lambda \sim 0.087$ Å^{-1}, this overestimation is 0.50–0.55 μ_B, which will only increase further as magnetic peaks at higher angles are considered. Therefore, the large difference between the two sets of refined magnetic moments of Ru^{5+} is largely a result of the different magnetic form factors used for this ion.

The measurements reported here also go much further than the earlier studies as not only are lower temperatures studied, but also many diffraction patterns below the transition temperature were measured. As the lowest temperature they measured was 10 K, with a

lower flux instrument, the (001) peak was not observed in Sr_2HoRuO_6 and the component of the magnetic moment in the *ab* plane was omitted [9]. The *ab* component persists to 25 K in Sr_2TbRuO_6, so it was noted in their 10 K study of this material. The large discrepancy between the refined moment of 4.98(12) μ_B of Tb^{3+} found for Sr_2TbRuO_6 [13] and the theoretical value of 9.72 μ_B was explained by assuming further ordering of this moment below the measuring temperature of 10 K. Our results (figure 9) show that the ordered magnetic moment of Tb^{3+} is saturated at ∼14 K with ∼4.5 μ_B and so the discrepancy is real. Our variable temperature data showed that for both systems the rare earth and ruthenium sublattices ordered at coincident temperatures, the first observation of this important result. The temperature dependences of the refined magnetic moments (figures 8 and 9), which derive directly from the intensities of the magnetic peaks with temperature (figure 5), allow information on the magnetic interactions to be extracted.

3.2.3. Magnetic interactions. The magnetic structure, ordering temperature, magnetic profile with temperature and saturated magnetic moment size are very similar for the Ru^{5+} ions in Sr_2HoRuO_6 and $Sr_2YRu_{1-x}Cu_xO_6$ ($x = 0.15$) [15]. This indicates that for Sr_2HoRuO_6, the Ru–O–O–Ru antiferromagnetic interaction controls the ordering of the Ru^{5+} sublattice, and it is of the same strength in the Ho and Y materials. In the yttrium compounds, any tilting of the oxygen octahedra was determined to lower the magnetic ordering temperature. As the Ru–O–Y and Ru–O–Ho bond angles, which determine the tilting as the octahedra are reasonably regular, are both in the range of 154°–158°, this similarity of strengths between the two systems is to be expected. This successfully explains the ordering of the ruthenium, but not that of the holmium sublattice.

If the holmium sublattice were completely independent of the ruthenium sublattice, then the Ho^{3+} ions would order at a temperature determined by the strength of the Ho–O–O–Ho magnetic interaction. As Ho_2O_3 is paramagnetic [16] and the Ho–O–O–Ho interaction is expected to be even weaker (than Ho–O–Ho), this interaction can be neglected. Rather, for the holmium sublattice to order there must be an *inter-species* interaction between the Ru^{5+} and Ho^{3+} ions, which is antiferromagnetic in nature as the sublattices are anti-parallel to each other (figure 6(b)). This Ru–O–Ho magnetic interaction will only result in the ordering of the holmium sublattice once the ruthenium sublattice is itself ordering, and explains the coincident ordering temperatures of the Ru^{5+} and Ho^{3+} ions, as first shown by these measurements.

Any Ru–O–Ho interaction will raise the ordering temperature of the ruthenium (and holmium) sublattice due to the Ru–O–Ho–O–Ru interaction. As Sr_2HoRuO_6 orders at 34 K, only marginally higher than the 33 K for the Y compound, which has no supporting Ru–O–Y–O–Ru interaction [15], the Ru–O–Ho interaction must be relatively weak. In the case of a weak *inter-species* interaction the saturation temperatures of the Ru^{5+} and Ho^{3+} magnetic moments, at 20 and 4 K respectively, provide a good estimate of the ratio of the strengths of the magnetic interactions. This is because once the ruthenium sublattice is fully ordered at 20 K, the only limitation on the ordering of the holmium sublattice is the strength of the Ru–O–Ho interaction. Thus, the more gradual ordering of the Ho^{3+} magnetic moments is due to the effect of the Ru–O–Ho magnetic interaction being a factor of 5 times weaker than the Ru–O–O–Ru magnetic interaction in the material. Each Ru^{5+} ion has 12 NNN Ru^{5+} and 6 NN Ho^{3+} ions and so an individual Ru–O–O–Ru interaction is only a factor of 2.5 times stronger than an individual Ru–O–Ho interaction.

The magnetic interactions present in Sr_2TbRuO_6 can also be determined in a similar manner. The Tb–O–O–Tb interaction is thought to be very weak due to the very low Néel temperature of Tb_2O_3 of 2.4 K [17, 18] and so the Ru–O–O–Ru and Ru–O–Tb antiferromagnetic interactions are the only ones of significance. As the Ru–O–Ln bond angles,

which are a measure of the octahedral tilting, are the same in the Ho and Tb compounds, the Ru–O–O–Ru interaction is expected to be of the same strength in the two systems. This explains the reasonably similar behaviours of the Ru^{5+} magnetic moment in Sr_2HoRuO_6 and Sr_2TbRuO_6. However, the elevated saturation and ordering temperatures of Ru^{5+} at 25 and 39 K in the Tb material indicate that the ruthenium sublattice has received additional support. This arises from the Ru–O–Tb–O–Ru interaction and suggests that the Ru–O–Tb interaction is substantially stronger than the Ru–O–Ho interaction.

Further evidence for a stronger Ru–O–Tb interaction arises from the refinements of the Tb^{3+} magnetic moment itself, particularly the higher saturation temperature of $\sim$14 K for these ions. The temperature dependence of the refined magnetic moment of Tb^{3+} is also more similar to that of Ru^{5+}, which suggests that the ordering of the terbium sublattice by the Ru–O–Tb interaction is partially limited by the ordering level of the ruthenium sublattice. This suggests that the Ru–O–O–Ru and Ru–O–Tb interactions are reasonably similar in strength in the materials. However, the direct ratio of the saturation temperatures of the Ru^{5+} and Tb^{3+} ions will not give a good estimate of the relative strengths of these two interactions, as the ruthenium sublattice is partially supported by the Ru–O–Tb interaction via the Ru–O–Tb–O–Ru pathway. As the Ru–O–O–Ru interaction is of the same strength in the Ho material as in the Tb material and leads to a saturated Ru^{5+} moment at 20 K in Sr_2HoRuO_6, its ratio with the $\sim$14 K saturation temperature of the Tb^{3+} magnetic moments will provide a better estimate of the relative interaction strengths. Thus, the effect of the Ru–O–O–Ru interaction is a factor of $\sim$1.4 times stronger than the Ru–O–Tb interaction in Sr_2TbRuO_6. As there are twice as many Ru–O–O–Ru interactions as Ru–O–Tb interactions, the strength of an individual Ru–O–O–Ru interaction is a factor of $\sim$0.7 of the strength of an individual Ru–O–Tb interaction.

4. Conclusions

This study has utilized both high-resolution and high-flux neutron powder diffraction to refine the crystal and magnetic structures of Sr_2LnRuO_6 (Ln = Ho or Tb). The power of variable temperature neutron diffraction was highlighted, as it allowed many diffraction patterns below the magnetic ordering temperature to be measured in a short amount of beam-time, enabling the system of magnetic interactions in the materials to be determined.

The crystal structures have been determined as distorted double perovskites which do not change significantly through the magnetic ordering transition at 30–40 K. Below this temperature, both the Ru^{5+} and Ln^{3+} magnetic moments adopt interpenetrating Type I antiferromagnetic structures, which are arranged anti-parallel to each other. The moments are primarily in the *c*-direction, though a small *ab* component is measurable at the lowest temperatures.

In the Sr_2LnRuO_6 system, the rare earth and the ruthenium sublattices order at a coincident magnetic ordering temperature, with the behaviours of the magnetic moment of Ru^{5+} reasonably similar in the two compounds and saturating at 20 or 25 K with 1.7–1.9 μ_B. The Ho^{3+} magnetic moments order more gradually and finally saturate at $\sim$4 K with $\sim$8 μ_B. In the terbium compound, the Néel temperature and saturation temperatures of both ions are higher, with the Tb^{3+} magnetic moments saturating at 14 K with $\sim$4.5 μ_B.

The magnetic structures and their development with temperature can be explained by antiferromagnetic Ru–O–O–Ru and Ru–O–Ln interactions, while the Ln–O–O–Ln interaction is negligibly weak. From the ratio of the appropriate saturation temperatures the relative strengths of the interactions in the materials could be deduced. The Ru–O–O–Ru interactions are of approximately the same strength in the materials and are factors of $\sim$2.5 and $\sim$0.7 times stronger than the Ru–O–Ln interactions in the Ho and Tb materials respectively.

Acknowledgments

The authors wish to thank both the ILL and ISIS facilities for the provision of beam-time and technical assistance. NGP is grateful to EPSRC for a studentship and also St Aidan's College, Durham, for the Beatrice Hollingworth scholarship. PDH thanks the University of Durham for the award of a Sir James Knott Foundation Fellowship. JAKH thanks the EPSRC for the award of a Senior Research Fellowship.

References

[1] Battle P D and Macklin W J 1984 *J. Solid State Chem.* **52** 138–45
[2] Battle P D, Gibb T C, Jones C W and Studer F 1989 *J. Solid State Chem.* **78** 281–93
[3] Doi Y, Hinatsu Y, Nakamura A, Ishii Y and Morii Y 2003 *J. Mater. Chem.* **13** 1758–63
[4] Anderson M T, Greenwood K B, Taylor G A and Poeppelmeier K R 1993 *Prog. Solid State Chem.* **22** 197–233
[5] Battle P D and Jones C W 1989 *J. Solid State Chem.* **78** 108–16
[6] Battle P D, Jones C W and Studer F 1991 *J. Solid State Chem.* **90** 302–12
[7] Doi Y and Hinatsu Y 1999 *J. Phys.: Condens. Matter* **11** 4813–20
[8] Larson A C and Von Dreele R B 2000 General structure analysis system (GSAS) *Los Alamos National Laboratory Report* LAUR 86-748
[9] Doi Y, Hinatsu Y, Oikawa K-I, Shimojo Y and Morii Y 2000 *J. Mater. Chem.* **10** 797–800
[10] Doi Y, Hinatsu Y, Oikawa K-I, Shimojo Y and Morii Y 2001 *J. Alloys Compounds* **323/324** 455–9
[11] Battle P D, Goodenough J B and Price R 1983 *J. Solid State Chem.* **46** 234–44
[12] Brown P J 1995 *The International Tables of Crystallography* vol C, ed A J C Wilson (Dordrecht: Kluwer) pp 391–9
[13] Doi Y, Hinatsu Y, Oikawa K-I, Shimojo Y and Morii Y 2000 *J. Mater. Chem.* **10** 1731–5
[14] Izumiyama Y, Doi Y, Wakeshima M, Hinatsu Y, Shimojo Y and Morii Y 2001 *J. Phys.: Condens. Matter* **13** 1303–13
[15] Parkinson N G, Hatton P D, Howard J A K, Ritter C, Chien F Z and Wu M K 2003 *J. Mater. Chem.* **13** 1468–74
[16] Schille J P, Sainctavit P, Cartier C, Lefebvre D, Brouder C, Kappler J P and Krill G 1993 *Solid State Commun.* **85** 787–91
[17] Gerstein B C, Jelinek F J and Spedding F H 1962 *Phys. Rev. Lett.* **8** 425
[18] Hill R W 1986 *J. Phys. C: Solid State Phys.* **19** 673–82